Estimating fill factor and equivalent insulation thermal conductivity in AC contactor coils using hotspot temperatures and bayesian neural networks

Son Nguyen Thanh*, Tu Pham Minh, Anh Hoang, Tu Nguyen Hoang Anh

[1]*Hanoi University of Science and Technology*
**Corresponding author. Email: son.nguyenthanh@hust.edu.vn*
DOI: https://doi.org/10.64032/mca.v30i2.398

Abstract

This study introduces a Bayesian neural network (BNN)-based framework for non-invasively estimating two fundamental insulation-related parameters of AC contactor coils: the fill factor and the equivalent thermal conductivity, using measured hotspot temperatures as the primary diagnostic input. Together, these parameters play a crucial role in determining the coil's temperature rise, thermal stability, and long-term reliability. However, accurately determining them through direct measurement is often difficult or impractical, particularly for compact contactor coils, where disassembly can damage the winding or may be impossible without specialized instruments. To address this challenge, the finite element method (FEM) is employed to model the coil's temperature distribution under varying insulation conditions, thereby generating a comprehensive and physically grounded dataset for training the BNN. In the proposed method, hotspot temperatures, which are obtained indirectly from measured ambient conditions and coil surface temperatures, serve as the inputs from which the BNN predicts the corresponding fill factor and equivalent thermal conductivity. By eliminating the need for coil teardown or complex laboratory procedures, this approach offers a practical, data-driven solution for evaluating coil design, diagnosing insulation characteristics, optimizing thermal management strategies, and ultimately enhancing the reliability and performance of electromechanical switching devices.

***Keywords**: AC contactor coil; Fill factor; Thermal conductivity; Finite element method; Bayesian neural networks.*

Abbreviations

AC	Alternating current
BNN	Bayesian neural network
FEM	Finite element method
FFN	Feedforward neural network

1. Introduction

AC contactors are electromechanical switching devices used to connect or disconnect AC electrical power to a load, enabling remote, frequent, and safe control of high-current circuits [1, 2]. They operate by using an energized coil to actuate movable contacts, allowing control signals to switch large loads without direct human interaction. In addition to basic switching, AC contactors enhance system safety by providing electrical isolation and reducing the need for manual operation of high-voltage equipment.

Research on AC contactors primarily focuses on enhancing their electrical, thermal, and mechanical performance to ensure reliable and long-lasting operation in various industrial applications. Particular attention has been given to contact wear [3], which directly affects the electrical life of the device due to repeated arcing and mechanical friction during switching. In addition, some studies have investigated arc behavior [4, 5], including arc formation, extinction, and the resulting impact on contact erosion and insulation degradation. Another critical area of research is coil heating [6], as excessive thermal buildup can reduce the magnetic efficiency of the coil, compromise insulation integrity, and shorten both the electrical and mechanical life of the contactor. Collectively, these research efforts aim to optimize contactor design, improve durability under heavy or inductive loads, and enable safer and more efficient operation in complex electrical systems.

The initial characteristic parameters of AC contactors can be used to estimate their electrical life [7], as these parameters provide a baseline for assessing contact and coil performance under rated conditions. In addition, the residual electrical life of a contactor can be predicted using electrical performance degradation models [8], which consider factors such as contact wear, arcing, and coil heating over time. More recently, AI-based methods have been developed to improve the prediction of AC contactor electrical endurance, enabling more accurate estimation of lifespan by analyzing large datasets of operational and environmental conditions [9]. These approaches allow for predictive maintenance, optimized operation, and enhanced reliability in industrial electrical systems.

Finite element method (FEM) is a powerful computational tool widely used in the analysis and design of AC contactors [10]. It enables detailed simulation of the contactor's electromagnetic, thermal, and mechanical behavior, which is difficult to assess accurately with analytical methods alone. Using FEM, engineers can predict the magnetic flux distribution in the coil and core, calculate the pull-in and release forces of the moving contacts, and optimize coil design for minimal energy consumption. Thermal simulations allow evaluation of temperature rise in the coil due to winding losses, assess heat dissipation efficiency, and ensure insulation and materials can withstand operational conditions.

The fill factor and equivalent thermal conductivity of an AC contactor coil strongly affect its temperature rise. A lower fill factor, representing less copper per coil volume, increases resistance and heat generation, while higher thermal conductivity enhances heat dissipation. Together, these parameters determine the coil's thermal performance, insulation life, and overall electrical lifespan, making their accurate estimation crucial for reliable operation.

By estimating the fill factor and equivalent thermal conductivity from measurable data such as hotspot

Received: 29 November 2025; Revised: 19 March 2026; Accepted: 19 March 2026.

temperature, this approach enables engineers to assess the thermal condition of existing contactor coils without disassembly. It helps identify overheating risks, insulation degradation, and inefficient heat transfer, while supporting maintenance, diagnostics, and safe operation assessment. Consequently, the method enhances thermal monitoring, fault detection, and reliability evaluation, contributing to extended service life and stable operation of existing AC contactors.

In this study, Bayesian neural network (BNN) is used to find the fill factor and the equivalent thermal conductivity of the AC coil insulation based on the empirical method for finding the hotspot temperature inside the AC contactor coil. A BNN models its weights and biases as probability distributions, enabling it to provide predictions together with uncertainty estimates. This probabilistic framework improves robustness to noise, reduces overfitting, enhances generalization with limited data, and offers more reliable and interpretable outputs compared to standard deterministic neural networks [11, 12]. Moreover, an effective approach that integrates simulation and experimental data is developed to estimate the fill factor and the equivalent thermal conductivity of the insulation in an AC contactor coil. FEM analysis is used to obtain the temperature distribution within the coil and to generate the training dataset for the BNN. After training, the BNN can accurately predict both the fill factor and the equivalent thermal conductivity of the coil insulation.

The paper is organized as follows. Section 2 presents the thermal analysis of the AC contactor coil. Section 3 provides a detailed description of the BNN. Section 4 outlines the simulation and experimental procedures. Section 5 concludes the study and discusses potential future work.

2. Thermal analysis of the AC contactor coil

An AC contactor coil is the electromagnetic component responsible for generating the magnetic force that closes the contactor's main contacts. When an AC voltage is applied to the coil, alternating current flows through its windings, producing a time-varying magnetic field that energizes the magnetic core and pulls the movable armature toward the fixed core. This action closes the power contacts and enables current flow to the load. When the supply is removed, the magnetic field collapses, the return spring releases the armature, and the contacts open.

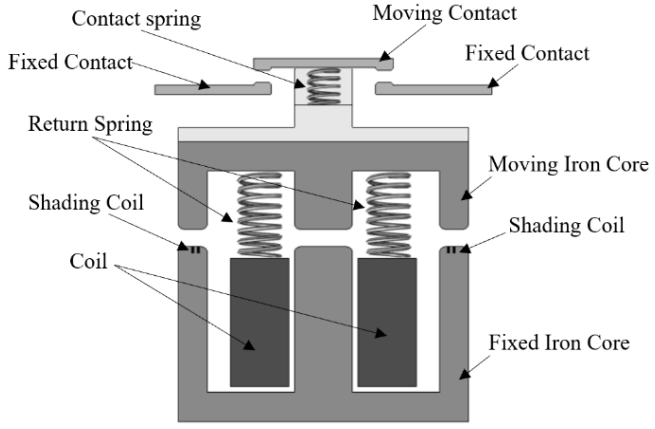

Figure 1: Key components of an AC contactor.

Figure 1 shows several key components that work together to control the switching of electrical circuits. The coil (solenoid winding) generates a magnetic field when energized by an AC supply, which produces the force needed to move the armature. The magnetic core (fixed iron core), usually made of laminated soft iron, provides a low-reluctance path for the magnetic flux and directs it toward the movable part. The armature (moving iron core) is attracted to the fixed iron core when the coil is energized, causing the contacts to close and complete the electrical circuit.

2.1 Thermal parameters of the coil in heat conduction

Figure 2 illustrates the core and coil of the AC contactor investigated in this study. The magnetic core adopts an EI-type laminated structure, which is widely used in electromagnetic devices due to its ease of assembly and effective magnetic flux distribution. The coil is composed of a bobbin and enamel-insulated copper windings, where the bobbin provides mechanical support and electrical insulation, while the copper conductors generate the magnetic field when energized. This configuration ensures reliable electromagnetic performance and facilitates efficient heat dissipation during operation.

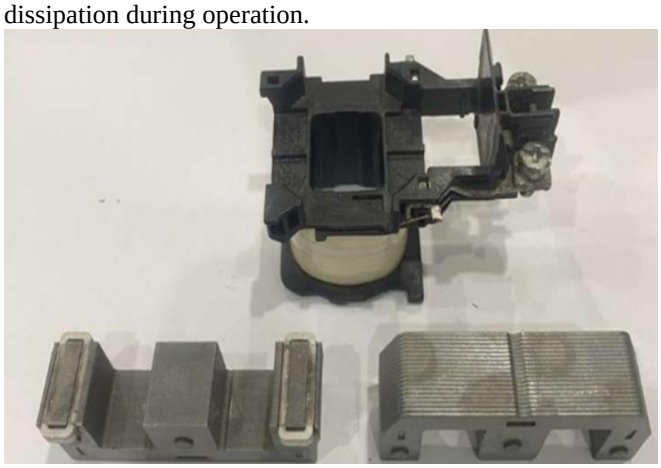

Figure 2: The core and coil of the AC contactor in this study.

Due to geometric symmetry about two orthogonal axes, only one-quarter of the AC contactor coil cross-section is analyzed, as illustrated in Figure 3. This simplification significantly reduces computational effort while preserving the accuracy of the thermal analysis. The outer surface of the coil is directly exposed to the ambient environment and is therefore subject to convective and radiative heat transfer, whereas the inner surface is in thermal contact with the bobbin, which influences heat dissipation toward the core structure. The coil cross-section consists of alternating layers of copper conductors and insulation materials, forming a heterogeneous composite structure. Because copper and insulation exhibit significantly different thermal properties, particularly in terms of thermal conductivity and heat capacity, heat transfer within the coil is inherently non-uniform. Thermal energy generated by Joule losses in the copper windings is conducted through both the conductors and the surrounding insulation, creating complex heat flow paths.

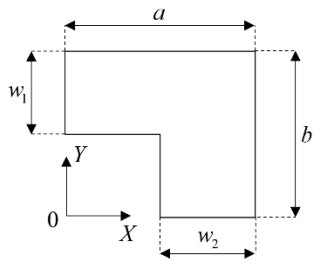

Figure 3: One-fourth of the cross-section of an AC contactor coil.

Since copper and insulation have very different thermal conductivities, heat transfer through the coil cannot be described by copper alone. Instead, an equivalent thermal conductivity can be computed as follows [15]:

$$\frac{1}{k_{eq}} = \frac{f_{cu}}{k_{cu}} + \frac{1-f_{cu}}{k_{ins}} \quad (1)$$

where:

k_{eq} : equivalent thermal conductivity of the coil $\left[W/m.K\right]$,

$k_{cu} \approx 385 \div 401 \left[W/m.K\right]$: thermal conductivity of copper,

$k_{ins} = 0.1 \div 0.9 \left[W/m.K\right]$: thermal conductivity of insulation,

f_{cu} : fill factor.

For the 2D FEM-based analysis of the temperature distribution in the AC contactor coil, the equivalent thermal conductivity in both principal axes can be considered identical. This assumption is justified by the geometric and material symmetry of the coil, which allows its thermal properties to be treated as isotropic within the analyzed plane. Therefore, the equivalent thermal conductivity used in the FEM model can be expressed as follows [13, 15]:

$$k_x = k_y = k_{eq} \quad (2)$$

The volumetric heat capacity of a material is calculated as follows [15]:

$$C_v = \rho c_p \quad (3)$$

where:

ρ : Density of material $\left[kg/m^3\right]$,

c_p : Specific heat capacity the material $\left[J/kg.K\right]$,

C_v : Volumetric heat capacity of material $\left[J/m^3.K\right]$.

The equivalent volumetric heat capacity of the entire AC contactor coil is determined as follows [15]:

$$C_{v,eq} = f_{cu} C_{v,cu} + \left(1-f_{cu}\right) C_{v,ins} \quad (4)$$

where:

$C_{v,eq}$: Equivalent volumetric heat capacity $\left[J/m^3.K\right]$,

$C_{v,cu}$: Volumetric heat capacity of copper $\left[J/m^3.K\right]$,

$C_{v,ins}$: Volumetric heat capacity of insulation $\left[J/m^3.K\right]$.

2.2 Thermal parameters of the coil in heat conduction

In heat-flow analyses of AC contactor coils, the general heat-conduction equation is commonly employed to describe the temperature distribution within the coil material. The equation is expressed as follows [13]:

$$\rho c \frac{\partial T}{\partial t} = \nabla.\left(k \nabla T\right) + Q \quad (5)$$

where:

T : Temperature $\left[K\right]$,

ρ : Density $\left[kg/m^3\right]$,

c : Specific heat $\left[J/kg.K\right]$,

k : Thermal conductivity $\left[W/m.K\right]$,

Q : Volumetric heat generation $\left[W/m^3\right]$.

FEM is a numerical technique used to determine temperature distribution and heat flow in solid bodies with complex geometries, materials, and boundary conditions. In FEM, the domain is divided into small elements, and temperature within each element is approximated using shape functions, converting the heat-conduction differential equation into algebraic equations. These element equations are assembled into a global system, boundary conditions such as specified temperature, heat flux, or convection are applied, and the resulting linear system is solved to obtain nodal temperatures. From these, temperature gradients and heat-flux fields are computed, enabling accurate analysis of steady-state or transient thermal behavior.

The volumetric heat generation is computed based on the sampled voltage applied to the coil and the current flowing through the coil, as follows:

$$Q = \frac{1}{V}\left(\frac{1}{N}\sum_{n=1}^{N} V_n I_n\right) \quad (6)$$

where:

V_n : The n -th sampled voltage applied to the coil $\left[V\right]$,

I_n : The n -th sampled current flowing in the coil $\left[A\right]$,

N : Number of samples of the voltage and current,

V : Volume of the coil $\left[m^3\right]$.

In heat conduction analysis using the FEM, the governing equation must be supplemented with appropriate boundary conditions (BCs) to obtain a unique solution for the temperature field. The most common types of boundary conditions are as follows [13]:

1) Fixed temperature

$$T = T_0 \quad (7)$$

in which T and T_0 are absolute temperatures $\left[K\right]$.

2) Heat flux

$$q = -k\frac{\partial T}{\partial n} \quad (8)$$

where:

q : Heat flux $\left[W/m^2\right]$,

k : Thermal conductivity $\left[W/m.K\right]$,

$\frac{\partial T}{\partial n}$: Temperature gradient $\left[K/m\right]$.

3) Convection

$$q = h\left(T - T_\infty\right) \quad (9)$$

where:

q : Heat flux $\left[W/m^2\right]$,

h : Convection coefficient $\left[W/m^2.K\right]$,

T_∞ : Steady-state temperature $\left[K\right]$,

$T - T_\infty$: Temperature difference $[K]$.

4) Radiation

$$q = \varepsilon\sigma\left(T^4 - T_{surface}^4\right) \tag{10}$$

where:

q : Heat flux $\left[W / m^2\right]$,

ε : Emissivity $[-]$,

σ : Stefan-Boltzmann constant $\left[5.67\times10^{-8} W / m^2 K^4\right]$,

$T, T_{surface}$: Absolute temperatures $[K]$.

2.3 Finite element method magnetics

In this study, Finite Element Method Magnetics (FEMM), an open-source software package, was used to solve two-dimensional heat flow problems [13]. FEMM developed based on the FEM to compute electric, magnetic, and thermal field distributions with high accuracy. It is widely used in electrical engineering applications such as transformer modeling, motor design, inductors, contactors, and electromagnetic actuators. Owing to its capability to evaluate detailed thermal and magnetic distributions inside coils and ferromagnetic components, FEMM is particularly useful for generating training data for neural networks and validating analytical or empirical models.

FEMM offers seamless automation through its built-in Lua scripting engine, enabling users to programmatically create geometries, assign material properties, execute simulations, and extract results without manual interaction. This capability greatly improves efficiency, especially when generating large datasets or performing repetitive computations. In this study, Octave, which is a high-level numerical computing language like MATLAB, is used alongside FEMM to automatically generate model parameters and compute the empirical hotspot temperature of the AC contactor coil. The integration of Octave with FEMM's Lua scripting facilitates consistent, repeatable, and scalable data generation for training the neural network.

2.4 Hotspot temperature empirical estimation

Hotspots in an AC contactor coil typically occur in regions where current density, copper losses, or thermal resistance are highest. Hotspots often appear near the inner layers of the coil winding, where heat removal is limited, or around areas with concentrated magnetic flux that increases copper and eddy-current losses. Insulation materials and winding geometry can further restrict heat dissipation, causing localized temperature rise. During operation, these hotspots can accelerate insulation aging, reduce coil life, and affect the reliability of the contactor. Accurate prediction of hotspot temperature is essential for evaluating coil performance and ensuring safe thermal limits. The following empirical formula can be used to estimate the hotspot temperature:

$$T_{hotspot} = T_{surface} + k\left(T_{surface} - T_{ambient}\right) \tag{11}$$

where:

$T_{surface}$: Coil surface temperature $[K]$,

$T_{ambient}$: Ambient temperature $[K]$,

k : Empirical constant.

Since the hotspot temperature is directly influenced by both the fill factor and the equivalent thermal conductivity of the insulation, it serves as a key indicator of the coil's internal thermal behavior. Therefore, performing a detailed thermal analysis of the coil's temperature distribution using the FEM, combined with neural network-based modeling, enables the accurate estimation of these parameters.

3. Bayesian neural networks

BNNs can be viewed as an advanced form of traditional feedforward neural networks (FNNs), in which information flows strictly from the input layer to the output layer without any feedback connections. Each neuron computes a weighted sum of its inputs, adds a bias term, and applies a nonlinear activation function. This structure allows FNNs to learn and approximate complex input–output relationships, making them widely used for classification, regression, and pattern-recognition tasks.

The feedforward neural network (FFN) takes a vector of real inputs, x_i , and from them compute one or more values of activation of the output layer, $a_k\left(x, w\right)$. With a single hidden layer FNN, the activation of the output layer is computed as follows:

$$a_k\left(x\right) = b_k + \sum_{j=1}^{M} w_{kj} \tanh\left(\bar{b}_j + \sum_{j=1}^{d} \bar{w}_{ji} x_i\right) = b_k + \sum_{j=1}^{M} w_{kj} y_j \tag{12}$$

where $\bar{w}_{ji}$ is the weight on the connection from input unit i to hidden unit j ; similarly, w_{kj} is the weights on the connection from hidden unit j to output unit k . The $\bar{b}_j$ and b_k are the biases of the hidden and output units. These weights and biases are the parameters of the neural network. For regression problems, the activation function of the output units is a linear function as follows:

$$z_k\left(x\right) = a_k\left(x\right) \tag{13}$$

A data error function is defined as follows:

$$E_D = \frac{1}{2}\sum_{n=1}^{N}\sum_{k=1}^{c}\left(z_k^{(n)} - t_k^{(n)}\right)^2 \tag{14}$$

where:

$z_k^{(n)}$: The k -th true output corresponding to the n -th pattern,

$z_k^{(n)}$: The k -th target output corresponding to the n -th pattern,

c : Number of network output units,

N : Number of patterns in the network training dataset

In neural network training, regularization is used to avoid overfitting the network after being trained. Specifically, a weight function is defined to be added to the data error function as follows:

$$S = \beta E_D + \alpha E_W \tag{15}$$

where E_W is called the weight function, which has the following form:

$$E_W = \frac{1}{2}\|w\|^2 = \frac{1}{2}\sum_{i=1}^{W} w_i^2 \tag{16}$$

The purpose of introducing the weight function is to penalize excessively large weights and biases, which are often

associated with overfitting in neural networks. By adding this penalty term, the training process encourages the network to maintain smaller, more balanced parameter values. This helps the model generalize better with unseen data, reduces sensitivity to noise in the training set, and improves overall stability and robustness. Parameters α and β are referred to as regularization parameters (or hyperparameters), and they can be inferred using Bayesian inference during the network training process. By applying Bayes' rule, the probabilistic distribution of the weight vector of the network can be computed as follows:

$$p(w|D) = \frac{p(D|w)\,p(w)}{p(D)} \tag{17}$$

In which $p(w)$ is the prior distribution of the vector of weights and biases of the network, $p(D|w)$ is the dataset likelihood and $p(D)$ is known as the evidence, which is a normalization factor computed as follows:

$$p(D) = \int p(D|w)p(w)dw \tag{18}$$

In (15), α and β can be updated through iterative steps as follows:

$$\alpha = \frac{\gamma}{2E_W(w_{MP})} \tag{19}$$

$$\beta = \frac{N-\gamma}{2E_D(w_{MP})} \tag{20}$$

where w_{MP} is the most probable vector of weights and biases and γ is called the "well-determined parameter", which can be computed as follows:

$$\gamma = \sum_{i=1}^{W} \frac{\alpha}{\lambda_i + \alpha} \tag{21}$$

where $\lambda_1, \lambda_2, \mathrm{L}\ , \lambda_W$ are eigenvalues of the Hessian matrix $A = \nabla\nabla S(w)$.

The network training process aims to minimize the cost function via an iterative process of an appropriate optimization algorithm. The vector of weights is updated as follows:

$$w_{m+1} = w_m + \eta_m d_m \tag{22}$$

where:

w_m : Vector of weights and biases at the m-th iterative step,

w_{m+1} : Vector of weights and biases at the $m+1$-th iterative step,

d_m : Search direction at the $m+1$-th iterative step,

η_m : Learning rate at the $m+1$-th iterative step.

The conjugate gradient algorithm can be utilized to adaptively determine the search direction and learning rate. At the m-th iterative step, a "line search" is performed to find η_m as follows:

$$\eta_m = \frac{g_m^T d_m}{d_m^T A d_m} \tag{23}$$

where:

g_m : Gradient of the vector of weights and biases at the m-th iterative step,

d_m : Search direction at the m-th iterative step,

$A = \nabla\nabla S$: The Hessian matrix of the cost function.

The new search direction can be determined as follows:

$$d_{m+1} = -g_{m+1} + \beta_m d_m \tag{24}$$

where d_{m+1} is the search direction at the m-th iterative step and β_m is determined using the Polak–Ribiere as follows:

$$\beta_m = \frac{(g_{m+1} - g_m)^T g_{m+1}}{g_{m+1}^T g_m} \tag{25}$$

Newton's method can be seen as an alternative to the conjugate gradient method for fast optimization. The basic step of this optimization method is based on Newton's formula as follows:

$$w_{m+1} = w_m - A^{-1}(g_{m+1} - g_m) \tag{26}$$

However, the inverse Hessian matrix, $F = A^{-1}$, can be approximated using a class of algorithms called the quasi-Newton method such as the most successful Broyden, Fletcher, Goldfarb and Shanno (BFGS) method as follows:

$$F_{m+1} = F_m + \frac{pp^T}{p^T v} - \frac{(F_m v)v^T F_m}{v^T F_m v} + (v^T F_m v)uu^T \tag{27}$$

where p, v and u are as follows:

$$p = w_{m+1} - w_m\ ;\ v = g_{m+1} - g_m\ ;\ u = \frac{p}{p^T v} - \frac{F_m v}{v^T F_m v} \tag{28}$$

4. Bayesian neural networks

This section describes an experimental system used to measure electrical and thermal parameters of an AC contactor coil. As shown in Figure 4, the system consists of the following components:

- An AC contactor coil,
- AC voltage and current sensors,
- A National Instruments USB-6009 data acquisition (DAQ) device,
- A laptop running a graphical user interface (GUI)–based DAQ software developed using LabVIEW.

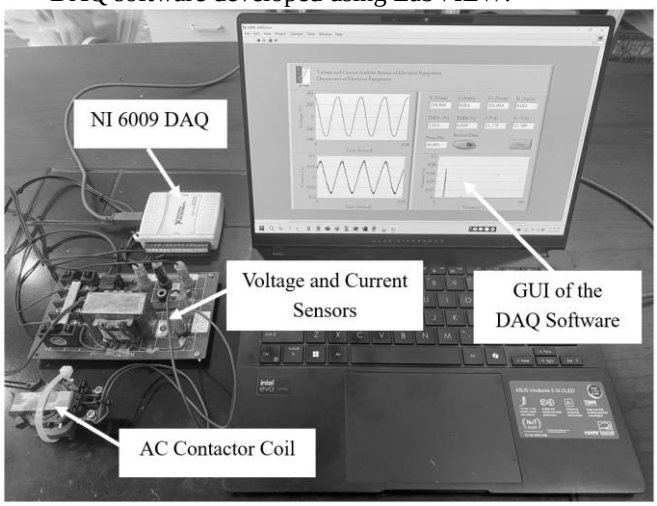

Figure 4: The electrical measurement system.

Figure 5 shows the GUI of the DAQ software, which provides the following functions:

- Displaying the waveform of the voltage applied to the coil,
- Displaying the waveform of the current flowing through the coil,
- Displaying the harmonic analysis of the coil current,
- Displaying the RMS value of the voltage applied to the AC contactor coil,
- Displaying the RMS value of the current flowing through the AC contactor coil,
- Displaying total harmonic distortion (THD) of the coil voltage and current,
- Saving the waveforms of the coil voltage and current for offline analyses using MATLAB.

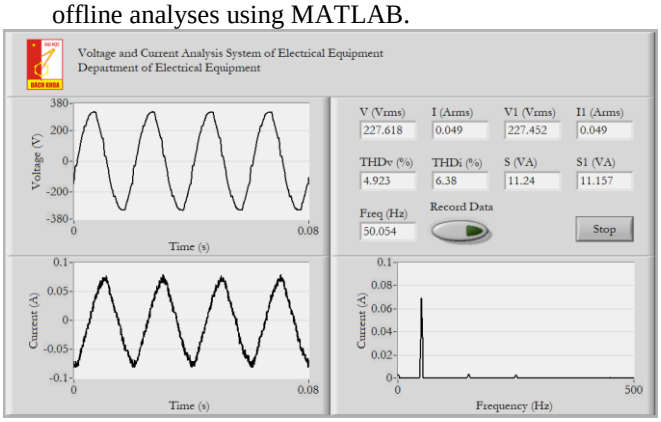

Figure 5: GUI of the DAQ software.

As shown in Figure 5, the coil current contains harmonic components introducing additional losses such as:

- Increased copper losses due to RMS current rise,
- Skin and proximity effects at higher frequencies,
- Possible additional eddy current losses in surrounding conductive parts.

As a result, the measured temperature inherently reflects both fundamental and harmonic loss contributions.

Table 1 presents the measured electrical parameters of the AC contactor coil, including voltage, current, active power, and related quantities. Among these parameters, active power plays a crucial role in the thermal evaluation of the coil. Specifically, it was used as the heat source for the FEM-based thermal analysis, ensuring that the simulated temperature distribution accurately reflects the actual power dissipation within the coil during operation.

Table 1: Electrical parameters of the AC contactor coil

Parameter	Value
RMS voltage (V)	227.1312
RMS current (A)	0.0480
Frequency (Hz)	50
Active power (W)	3.3405
Appearance power (VA)	10.9073
Resistance (Ω)	1448.6
Reactance (Ω)	4502.5

FEMM was employed to generate a comprehensive dataset required for training the FFN. By conducting steady-state thermal simulations across a wide range of insulation conditions—such as different fill factors and equivalent thermal conductivities, the software produced the corresponding hotspot temperatures for each parameter combination. This systematic variation of inputs allowed FEMM to capture the thermal behavior of the coil under diverse scenarios, ensuring that the resulting dataset was both rich and representative. The hotspot temperatures obtained from these simulations served as target outputs for training the FFN, enabling the network to learn the underlying thermal relationships between the coil's insulation properties and its temperature response.

The coil surface and ambient temperatures were measured using a UNI-T thermal camera, as shown in Figure 6. This handheld infrared device provides non-contact temperature readings and visualizes the temperature distribution of both the coil and its surrounding environment. The thermal image enables accurate identification of temperature variations across the coil surface.

The right-hand side of Figure 6 illustrates the heat distribution of the outer surface of the AC contactor coil. It should be noted that this figure does not represent the actual hotspot location within the coil. Since the highest temperature typically occurs within the inner layers of the winding-where heat dissipation is more limited-the surface heat map may not fully capture the true hotspot region. Nevertheless, it provides useful insight into the overall thermal behavior and surface temperature profile of the coil under steady-state conditions. Based on the recorded data, the coil surface temperature reached 66.1 °C, while the ambient temperature was approximately 26.6 °C. These temperature values are used to evaluate the thermal behavior of the coil in steady state.

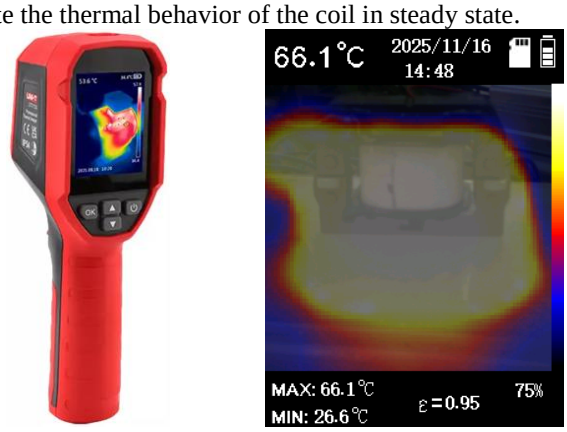

Figure 6: UNI-T thermal camera (left) and thermal image of the AC contactor coil surface at steady state (right).

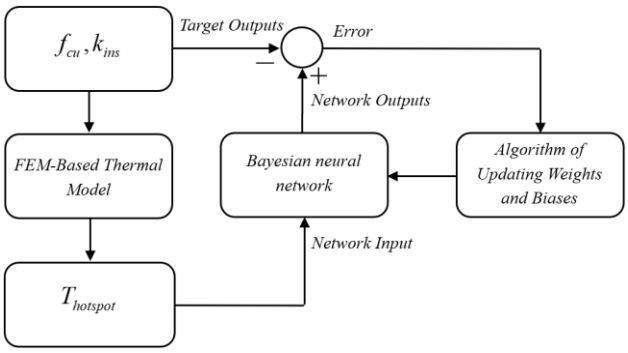

Figure 7: Principle of updating weights and biases of the BNN.

Figure 7 illustrates the principle of updating the weights and biases of the BNN. In this framework, the hotspot temperature is used as the input to the network, while the

outputs correspond to the estimated fill factor and equivalent thermal conductivity of the insulation. During the training process, the weights and biases are iteratively adjusted based on the discrepancy between the predicted outputs and the desired (target) values. This adjustment is typically performed using an optimization algorithm that minimizes a predefined cost function, ensuring that the network progressively improves its prediction accuracy. The iterative learning process continues until a stopping criterion is satisfied, which may be defined as reaching a maximum number of iterations or achieving an acceptable level of error between the network outputs and the target values. Through this procedure, the BNN is able to capture the underlying nonlinear relationships between hotspot temperature and the insulation properties of the coil.

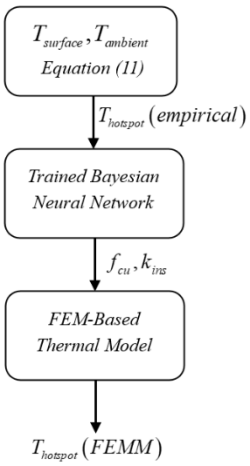

Figure 8: Principle of investigating the performance of the trained BNN using FEMM.

Figure 8 illustrates the principle of investigating the performance of the trained neural network. Firstly, the hotspot temperature, $T_{hotspot}$, was estimated based on the empirical equation (11). If $T_{surface} = 66.1^0C$, $T_{ambient} = 26.6^0C$ and $k = 0.1 \div 0.45$, then the range of the hotspot temperature varies from 70^0C to 82^0C.

Table 2 summarizes the ranges of the fill factor and equivalent thermal conductivity of the coil insulation. These parameters were used as inputs to the FEM-based thermal analysis model to obtain the resulting hotspot temperature. In this study, the dataset consists of 200 patterns.

Table 2: Ranges of parameters in the network training dataset

f_{cu}	$k_{cu}[W/m.K]$	$k_{ins}[W/m.K]$	$T_{hotspot}[^0C]$
$0.2 \div 0.5$	385	$0.1 \div 0.9$	$68 \div 82$

The BNN has the following architecture:

- One input node corresponding to the hotspot temperature,
- Ten units in the hidden layer,
- Two output nodes, which correspond to the fill factor and equivalent thermal conductivity of the coil.

The BFN was trained by following the procedure:

- **Step 1:** The network weights and biases were randomly initialized. Values of α and β were also chosen.
- **Step 2:** The weights and biases were updated through the minimization of the cost function using the quasi-Newton optimization method.
- **Step 3:** When the cost function had reached a local minimum or the number of iterative steps exceeded a specific value, the hyperparameters were re-estimated using (19), (20) and (21).
- **Step 4:** Repeating step 2 and 3 until the cost function will not change significantly in subsequent iteration.

Table 3 presents the changes in hyperparameters via five re-estimation periods.

Table 3: Changes of hyperparameters via the re-estimation period.

Period	β	α	γ
1	201.8273	0.0504	19.7213
2	202.3588	0.0488	17.8560
3	202.7977	0.0466	17.2312
4	202.6594	0.0473	17.8646
5	203.5654	0.0428	16.1564

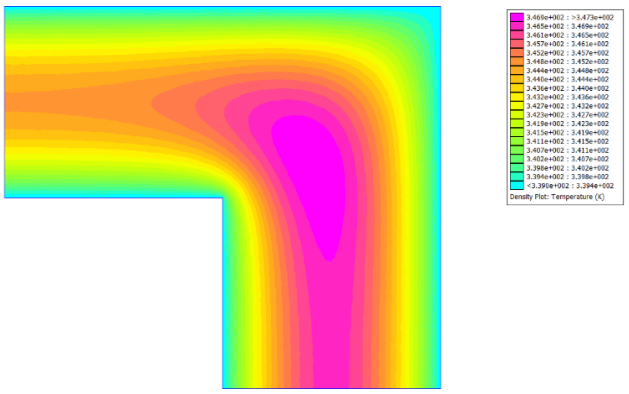

Figure 9: 2D FEM thermal analysis of one-quarter of the AC contactor coil.

Figure 9 illustrates the 2D FEM-based thermal analysis performed on one-quarter of the AC contactor coil, leveraging geometric symmetry to reduce computational effort while preserving accuracy. The resulting temperature distribution offers a detailed visualization of heat flow within both the winding and the surrounding insulation. This simulated thermal profile clearly reveals how heat is generated, conducted, and dissipated throughout the coil structure. From this 2D map, the hotspot region, where the temperature reaches its highest value, can be readily identified and tracked. Identifying this critical location provides essential insights into the coil's thermal performance, insulation integrity, and potential degradation mechanisms, thereby supporting more reliable condition evaluation and design optimization.

For a given hotspot temperature, the trained BNN can predict the corresponding fill factor and the equivalent thermal conductivity of the AC contactor coil insulation, as summarized in Table 4. Once these two key insulation parameters are estimated by the FFN, they are subsequently fed back into the FEM-based thermal analysis model to compute the resulting hotspot temperature under the inferred conditions. This two-step procedure with prediction followed

by FEM verification ensures that the estimated parameters are physically consistent with the thermal behavior of the coil.

Table 4: Estimation of the fill factor and thermal conductivity of the AC contactor coil insulation according to the hotspot temperatures.

$T_{hotspot}\left[{}^{0}C\right]$ Empirical estimation	f_{cu}	$k_{ins}\left[W/m.K\right]$	$T_{hotspot}\left[{}^{0}C\right]$ FEM-based thermal analysis
68	0.3916	0.7645	68.0270
70	0.2978	0.4367	69.9902
72	0.2947	0.2803	72.1862
74	0.3154	0.2087	74.0337
76	0.3245	0.1689	75.7721
78	0.3142	0.1404	77.9138
80	0.2896	0.1194	80.4899
82	0.2580	0.1069	82.8842

The proposed approach is adequate for engineering estimation, especially when harmonic content is moderate and similar to the conditions used for modeling. However, its accuracy may decrease for coils with very different geometries or in cases with strong or varying harmonics, since frequency-dependent losses are not included.

5. Conclusion

This study demonstrates that a BNN–based approach can effectively estimate the fill factor and the equivalent thermal conductivity of coil insulation in AC contactors using only hotspot temperature measurements. By combining FEM-generated thermal data with regression-based learning, the method bypasses the challenges associated with direct measurement of internal coil parameters, offering a practical and non-invasive alternative for condition evaluation. The results highlight the potential of data-driven techniques to support design optimization, thermal assessment, and reliability improvement in electromechanical switching devices.

Future research can further extend this approach in several directions. First, incorporating additional temperature- or geometry-related features may improve estimation accuracy and allow the model to generalize to a broader range of coil designs. Second, expanding the data set using 3D FEM simulations or experimental measurements from multiple AC contactor types could enhance robustness and applicability. Third, integrating the trained BNN into real-time monitoring systems for estimation of coil parameters under dynamic operating conditions. Finally, exploring hybrid models that combine physics-based methods with advanced machine learning techniques, such as physics-informed neural networks (PINNs), may provide deeper insights into coupled thermal-electromagnetic behavior and further improve predictive performance.

References

[1] Ye Tao, Qingquan Jia, Haiyan Dong, Shiwei Xue, Lingling Sun, Pan Li, “Tolerance Evaluating of AC Contactors to Irregular Sags With Differential Strategy,” IEEE Transactions on Power Delivery, vol. 37, no. 3, Jun. 2022, pp. 2413−2416, DOI: 10.1109/TPWRD.2022.3143357.

[2] Shuguang Sun, Jinfa Liu, Jingqin Wang, Fan Chen, Shuo Wei, Hui Gao, “Remaining Useful Life Prediction for AC Contactor Based on MMPE and LSTM With Dual Attention Mechanism,” IEEE Transactions on Instrumentation and Measurement, vol. 71, May. 2022, DOI: 10.1109/TIM.2022.3178994.

[3] Ziran Wu, Chufu Fang, Guichu Wu, Zhenquan Lin, Wei Chen, “A CNN-Regression-Based Contact Erosion Measurement Method for AC Contactors,” IEEE Transactions on Instrumentation and Measurement, vol. 71, Jul. 2022, DOI: 10.1109/TIM.2022.3192282.

[4] Zhe Zheng, Wanbin Ren, Tianyang Wang, “Experimental Investigation of the Breaking Arc Behavior and Interruption Mechanisms for AC Contactors,” IEEE Transactions on Plasma Science, vol. 49, no. 1, Jan. 2021, pp. 389−395, DOI: 10.1109/TPS.2020.3042545.

[5] Ziran Wu, Guichu Wu, Chong Chen, Yandong Fang, Lezhen Pan, Hailan Huang, “A Novel Breaking Strategy for Electrical Endurance Extension of Electromagnetic Alternating Current Contactors,” IEEE Transactions on Components, Packaging and Manufacturing Technology, vol. 6, no. 5, May. 2016, pp. 749−756, DOI: 10.1109/TCPMT.2016.2542101.

[6] Shuyi Lin, Xiaosheng Huang, “Power loss analysis of AC contactor with electromagnetic-thermal coupling method,” Journal of Information Hiding and Multimedia Signal Processing, vol. 8, no. 2, Mar. 2017, pp. 290–298.

[7] Shuguang Sun, Qiufu Wang, Taihang Du, Jingqin Wang, Senjuan Li, Junji Zong, “Quantitative Evaluation of Electrical Life of AC Contactor Based on Initial Characteristic Parameters,” IEEE Transactions on Instrumentation and Measurement, vol. 70, Oct. 2020, DOI: 10.1109/TIM.2020.3031160.

[8] Kui Li, Chengchen Zhao, Feng Niu, Shumei Zheng, Yu Duan, Shaopo Huang, “Electrical Performance Degradation Model and Residual Electrical Life Prediction for AC Contactor,” IEEE Transactions on Components, Packaging and Manufacturing Technology, vol. 10, no. 3, Mar. 2020, pp. 400−417, DOI: 10.1109/TCPMT.2020.2966516.

[9] Hechen Cui, Ziran Wu, Guichu Wu, Xiaofeng Xu, Yingmin You, Yandong Fang, “Convolutional Neural Networks for Electrical Endurance Prediction of Alternating Current Contactors,” IEEE Transactions on Components, Packaging and Manufacturing Technology, vol. 9, no. 9, Sep. 2019, pp. 1785−1793, DOI: 10.1109/TCPMT.2019.2930741.

[10] R. Gollee, A. Gerlach, “An FEM-based method for analysis of the dynamic behavior of AC contactors,” IEEE Transactions on Magnetics, vol. 36, no. 4, Jul. 2000, pp. 1337−1340, Jul. 2000, DOI: 10.1109/20.877686.

[11] C. M. Bishop, Neural Networks for Pattern Recognition. New York: Oxford Univ. Press, 1995.

[12] I. T. Nabney, NETLAB: Algorithms for Pattern Recognition. London: Springer, 2002.

[13] Finite Element Method Magnetics: https://www.femm.info/wiki/HomePage

[14] GNU Octave: https://octave.org/

[15] F. P. Incropera et al., Fundamentals of Heat and Mass Transfer, 7th ed., Wiley, 2011.